

EMD, EEMD, knee joint, vibration, kinetic chain

Anna MACHROWSKA [0000-0003-3289-2421]*,
Robert KARPIŃSKI [0000-0003-4063-8503]*,
Przemysław KRAKOWSKI [0000-0001-7137-7145]**,
Józef JONAK [0000-0003-4658-4569]*

DIAGNOSTIC FACTORS FOR OPENED AND CLOSED KINEMATIC CHAIN OF VIBROARTHROGRAPHY SIGNALS

Abstract

The paper presents results of preliminary research of vibroarthrography signals recorded from one healthy volunteer. The tests were carried out for the open and closed kinematic chain in the range of motion $90^\circ - 0^\circ - 90^\circ$. Analysis included initial signal filtration using the EMD algorithm. The aim was to investigate the occurrence of differences in the values of selected energy and statistical parameters for the cases studied.

1. INTRODUCTION

Anterior knee pain can be caused by multiple factors and is one of the most common complaints of the patients (Powers, Bolgla, Callaghan, Collins & Sheehan, 2012). However, etiology of the condition is still controversial (Sanchis-Alfonso, 2014). Chondromacia of articular cartilage in patellofemoral joint as well as increased forces in the joint are the most common causes of the pain (Sanchis-Alfonso & Dye, 2017). Up to this date there is no simple, fast, accessible and reproducible diagnostic modality to detect chondral lesions in patellofemoral joint. Vibroarthrography in future might bring a solution to this problem, however up to this date there is no standardized protocol of examination especially regarding patellofemoral joint.

* Lublin University of Technology, Faculty of Mechanical Engineering, Department of Machine Design and Mechatronics, , Nadbystrzycka 36, 20-618 Lublin, Poland, a.machrowska@pollub.pl, r.karpinski@pollub.pl, j.jonak@pollub.pl

** Orthopedic Department, Łęczna Hospital, Krasnystawska 52, 21-010 Łęczna, Poland

Open and closed kinetic chain in exercises is the terms introduced by Steindler in 1955 (Charnley, 1955). From that time, attention was brought to the stress distribution in knee joint during certain exercises. In closed kinetic chain distal segment of the limb is opposed by “considerable resistance” whereas in open kinetic chain the distal part of the limb is free to move without additional resistance. Closed kinetic chain exercises such as squats or leg presses imitate physiological movement patterns and involve cooperation between various muscle groups. In open kinetic chain it is possible to isolate one muscle group which needs strengthening. Therefore open and closed kinetic chain generates different loading patterns on patella-femoral and tibio-femoral joints (Adouni & Shirazi-Adl, 2009; Barcellona & Morrissey, 2016). Great attention was put into this phenomenon in relation to rehabilitation after ligamentous reconstructions, or anterior knee pain due to its stress distributions (Cohen et al., 2001; Luque-Seron & Medina-Porqueres, 2016; Witvrouw, Danneels, van Tiggelen, Willems, & Cambier, 2004). Stress distribution differs in patellofemoral joint during open and closed kinetic chain exercises depending on flexion angle of the joint (Cohen et al., 2001). In clinical setting open kinetic chain is easier to perform on standard examination, however up to this date, there is insufficient information about the differences in vibroacoustic signals emitted by patellofemoral joint in open and closed kinetic chain. Moreover, it is not known whether open or closed kinetic chain provides more accurate evaluation of anterior compartment of the knee joint (Karpiński, Machrowska, & Maciejewski, 2019).

The aim of the work was to determine statistical and energy indicators characterizing vibroarthrographic signals for an open and closed kinematic chain.

2. EMPIRICAL MODE DECOMPOSITION

Vibroarthrography (VAG) signals are inherently nonlinear and non-stationary. Failure in proper method and approach selection will invariably result in improper results and conclusion, which is further amplified due to complex and sensitive character of medical data as a whole (Maciejewski, 2015; Maciejewski, Surtel, & Dzida, 2015). Therefore, modern methods should be used for the analysis, allowing for proper interpretation of the results. A characteristic feature of the recorded VAG signals is the clear presence of low-frequency artifacts, which are the source of muscle tension, obtained during the tests (Luque-Seron & Medina-Porqueres, 2016). The methodology of knee joint state tests forces the limbs to flex and straighten, so it is not possible to exclude co-occurrence of muscle origin signals. For more accurate analysis of nonlinear and non-stationary VAG signals, the Empirical Mode Decomposition (EMD) algorithm was used. It allows the analysis of individual filtered signal components.

EMD is a popular signal processing method for the extraction of oscillation modes (Machrowska & Jonak, 2018). An unquestionable advantage of the algorithm is the possibility of using nonlinear and non-stationary input signals. The discussed tool has found a number of applications (Alickovic, Kevric & Subasi, 2018; Jonak, Machrowska, Podgórski & Bęc, 2016; Kolotkov, Anfinogentov & Nakariakov, 2016; Yaslan & Bican, 2017). As a part of the EMD procedure, the input signal is decomposed to a finite number of internal IMF (Intrinsic Mode Functions) components and a residual signal. The algorithm obtaining algorithm is based on the filtration process (sifting). In the input signal $x_1(t)$ local extremes are identified, then the signal envelope is constructed using interpolation with third order split functions (cubic spline). At each signal point, the average $m_1(t)$ and the difference between the input data $x(t)$ are determined (Huang et al., 1998):

$$h_1(t) = x(t) - m_1(t). \quad (1)$$

The $h_1(t)$ function is called intrinsic function (IMF) when it meets two conditions:

- (1) In the selected set of data, the number of extremes and the number of zero crossings of the function are equal to or differ at most by one,
- (2) At each point, the envelope's mean value defined by local maxima and minima is zero.

Sifting procedure is repeated k times, where $h_k(t)$ is given as an updated input signal:

$$h_k(t) = h_{k-1}(t) - m_k(t). \quad (2)$$

The filtration process is stopped when the condition of equality of zero crossings and local extremes is met. A residual signal $r_n(t)$ is then determined:

$$r_n(t) = x(t) - \sum_{i=1}^n c_i(t), \quad (3)$$

where $c_i(t)$ is the i^{th} internal function of IMF, while n is the highest possible number of modal oscillations. The residual signal $r_n(t)$ is then treated as an input signal for subsequent iterations. The sifting process is continued until the stoppage criterion is met. The basic condition for stopping is limitation of the standard deviation, determined for two successive results of the screening process. It is obtained on the basis of the equation (Huang et al., 1998):

$$SD = \frac{\sum_t |h_{i,k-1}(t) - h_{i,k}(t)|^2}{\sum_t h_{i,k-1}^2(t)}. \quad (4)$$

The sifting process ends when the SD value is less the pre-established initial one.

3. MATERIALS AND METHODS

The test were performed on a 23 years old white Caucasian male without knee joint disorders. The vibroarthrographic signal was recorded using a three-axis, miniature accelerometer sensor with Analog Devices ADXL325 analog output from the measuring range $\pm 5g$ per axis. The signal was sampled at 1000 Hz using an Texas Instruments analog measuring card connected to a PC. The sensor was attached to the skin using a double-sided adhesive tape about 1 cm above the top of the patella. The examination was carried out in a sitting position. The examined person had the task of extending and bending the raised limb in the range of $90^\circ - 0^\circ - 90^\circ$ (OKC). The study of motion in a closed kinetic chain (CKC) included alternating standing up and sitting on a chair (movement in the range of $90^\circ - 0^\circ - 90^\circ$). The diagram showing the directions of distribution of individual axes is shown in Figure 1.

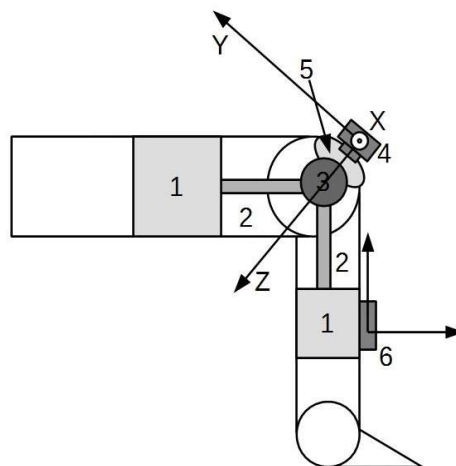


Fig. 1. Distribution of individual axes accelerometer sensor

4. RESULTS

Signal from the X axis resembles a sinusoidal waveform, for closed kinematic chain (CKC), the rise and fall times of the pulse slopes (movement in the concentric phase- muscle shortening and eccentric- muscle straightening) are definitely longer than for open kinematic chain (OKC). Above relationship is related to the longer motion range of the squatting with the CKC. The motion phases are also visible for the signal recorded in the Z axis. In the case of CKC, there are noticeable oscillations on the pulse crest, characteristic for knee locking after the concentric squat phase (Fig. 2 and Fig. 3). On the issue of OKC oscillations on

the pulse top are not so regular due to the fact of a short- term isometric contraction in the in the final movement phase (full extension of the limb). Mentioned vibrations are reflected in 3rd and 4th IMFs. High frequency IMFs 1st and the 2nd, on the other hand, shows filtered vibrations of the knee joints, crossed by unconsolidated peaks associated with the friction phenomenon, analogous to the slide bearings surfaces. The lower frequency IMFs do not have such a significant physical meaning.

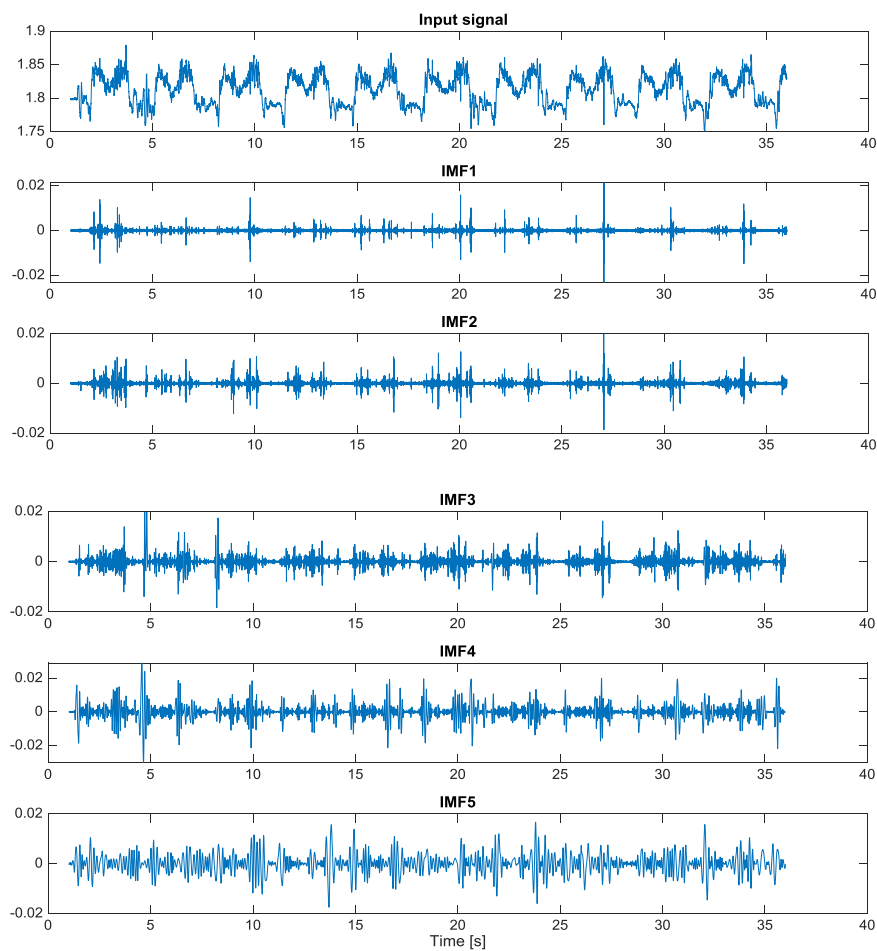


Fig. 2. Z axis – CKC

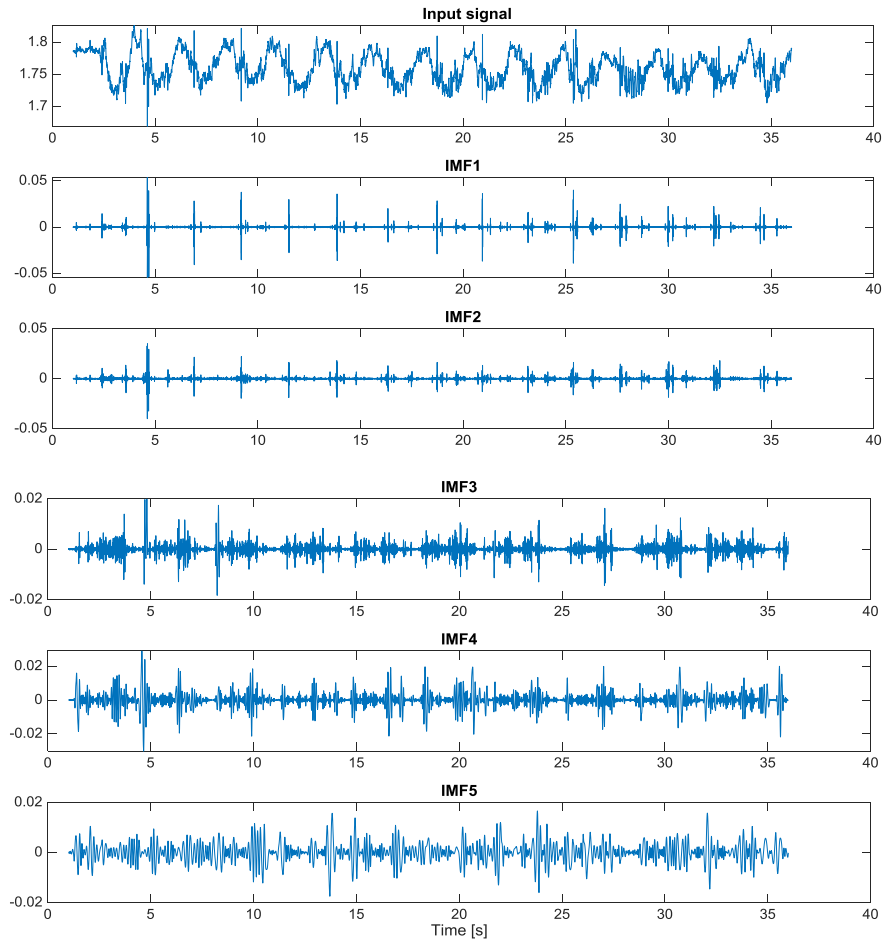


Fig. 3. Z axis – OKC

Signal energy is one of the most important factors to describe the signal. Values of signals energy for X axis is shown on figure 4. At higher frequencies, the energy values differ only slightly between OKC and CKC. In the lower frequency ranges (from IMF 6 up to 25 Hz) a closer differentiation of the signal energy value is visible. For the OKC energy values in the range of 10–25 Hz (IMF 6 and 7) are higher than for the CKC. The inverse relationship occurs at very low frequencies (from IMF 8).

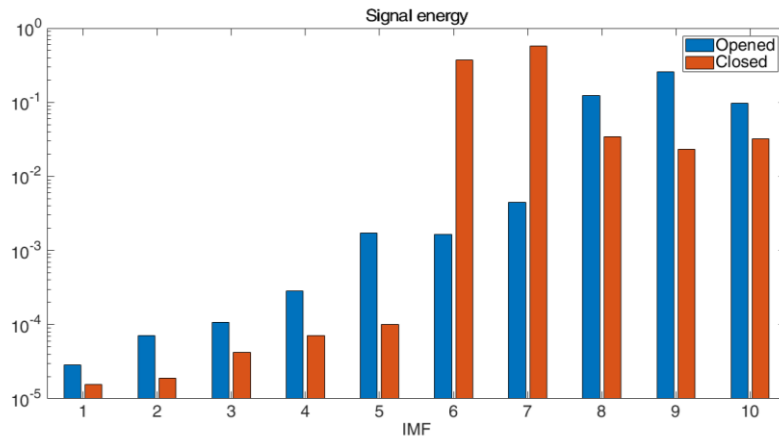


Fig. 4. X axis – signal energy for OKC and CKC

In the case of Y axis (Fig. 5), the highest signal energy values are observed in IMFs 5, 6 and 7 (15–30 Hz). In case of CKC, visible is tendency to taking higher values for higher frequency ranges in comparison to OKC. Thus the relationship between the transmission of joint structures vibration and type of kinematic chain is visible.

For Z axis (Fig. 6) higher values of the selected indicator are observed at low frequencies (IMF 7, 8 and 9), while the dependence of the occurrence of higher values for OKC is no longer as pronounced as for axes X and Y. There are no clear dominance of energy values for CKC in higher frequencies due to the sensor location.

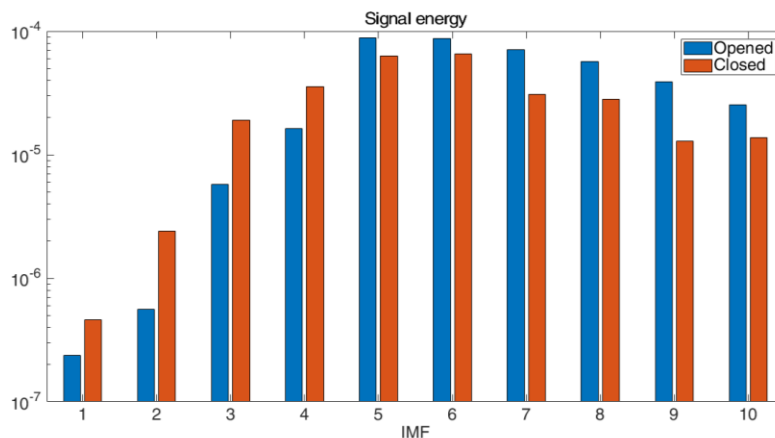


Fig. 5. Y axis – signal energy for OKC and CKC

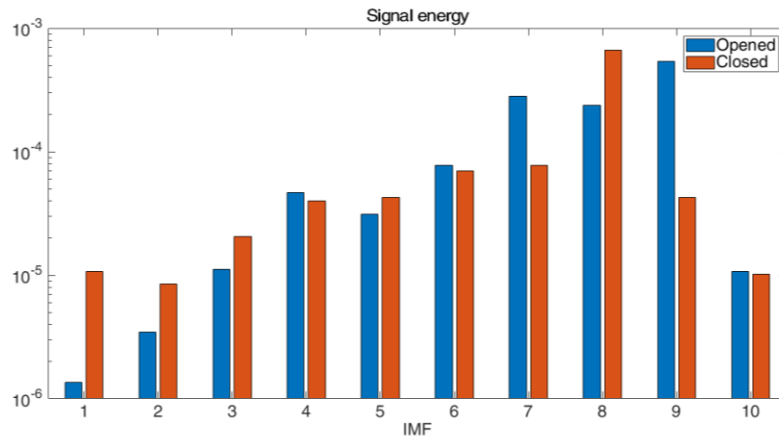


Fig. 6. Z axis – signal energy for OKC and CKC

Standard deviation parameter shows the scale of results scattering around the mean. Data from X axis (Fig. 7) are clearly more diverse for lower frequencies (IMF 6–10). For Y axis (Fig. 8) at higher frequencies (IMF 1–4), higher standard deviation values occur for CKC. The inverse relationship (higher standard deviation values for CKC) is visible in the lower frequency ranges (IMF 5–10). Above dependencies are not so clear the Z axis (Fig. 9) – higher indicator values can be only seen for higher frequencies (IMF 1–3), while for low frequencies the inverse relationship cannot be confirmed.

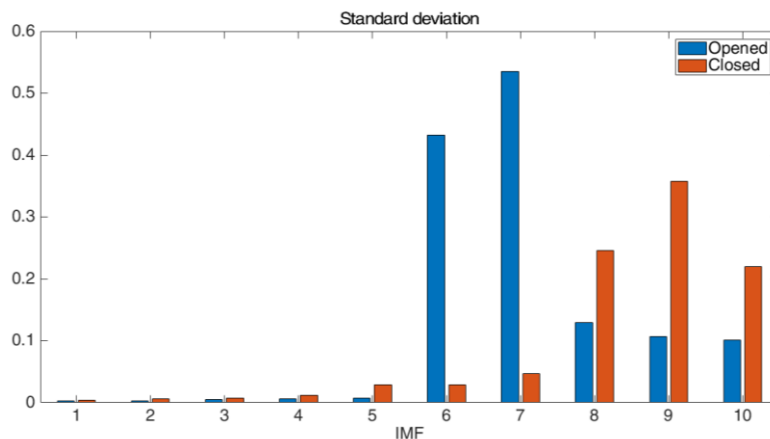


Fig. 7. X axis – standard deviation parameter for OKC and CKC

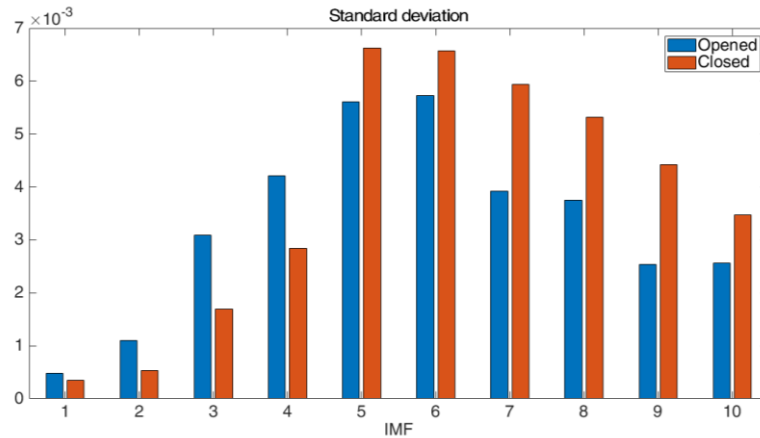


Fig. 8. Y axis – standard deviation parameter for OKC and CKC

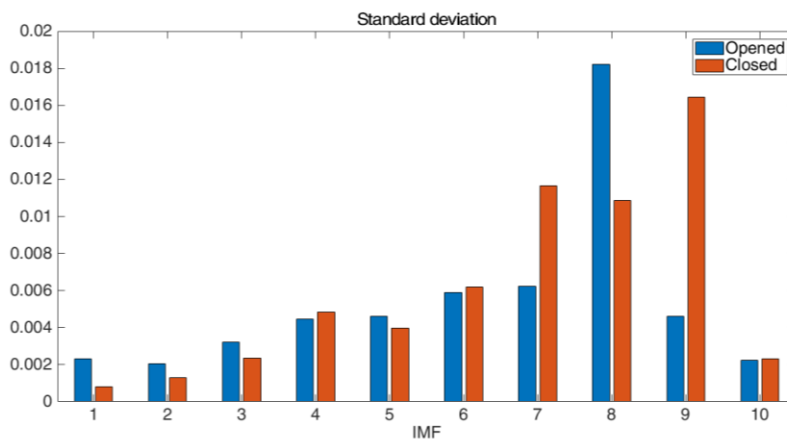


Fig. 9. Z axis – standard deviation parameter for OKC and CKC

5. CONCLUSIONS

The analysis of selected indicators of energy and statistical parameters allows to show the differences between the open and closed kinematic chain. An important factor is the correct positioning of the vibration sensor with the selection of the proper orientation of the sensor axis relative to the anatomical location (minimizing the attenuation of soft tissue and maximum use of bone conduction.)

The higher the signal energy at low frequencies in the Z axis for waveforms recorded in a closed kinematic chain due to the greater impact of vibration standard deviation takes higher values for signals recorded in the open kinetic chain.

The results obtained show that analysis in both the open and closed kinetic chains is important. Signal analysis for the open chain provides information related to the work of the unloaded limb, which allows a more accurate analysis of the functioning of cartilage structures due to the lower effect of muscle tension at high frequencies. In contrast, signal analysis for a closed kinetic chain provides us with information about the work of an anatomically loaded limb in real operating conditions.

Demonstrating the differences between the closed and open kinematic chains allows in the future a more accurate analysis and distinction of structures generating a vibroacoustic signal, which will allow analysis targeted at specific joint structures. Thanks to this analysis, it will be possible to assess the knee joint movement during walking, where signals generated by the open and closed kinematic chains overlap during walking.

REFERENCES

- Adouni, M., & Shirazi-Adl, A. (2009). Knee joint biomechanics in closed-kinetic-chain exercises. *Computer Methods in Biomechanics and Biomedical Engineering*, 12(6), 661–670. doi:10.1080/10255840902828375
- Alickovic, E., Kevric, J., & Subasi, A. (2018). Performance evaluation of empirical mode decomposition, discrete wavelet transform, and wavelet packed decomposition for automated epileptic seizure detection and prediction. *Biomedical Signal Processing and Control*, 39, 94–102. doi:10.1016/j.bspc.2017.07.022
- Barcellona, M. G., & Morrissey, M. C. (2016). The effect of open kinetic chain knee extensor resistance training at different training loads on anterior knee laxity in the uninjured. *Manual Therapy*, 22, 1–8. doi:10.1016/j.math.2015.12.011
- Charnley, J. (1955). Kinesiology of the human body under normal and pathological conditions. *The Journal of Bone and Joint Surgery. British Volume*, 37-B(4), 736–737. doi:10.1302/0301-620X.37B4.736
- Cohen, Z. A., Roglic, H., Grelsamer, R. P., Henry, J. H., Levine, W. N., Van Mow, C., & Ateshian, G. A. (2001). Patellofemoral Stresses during Open and Closed Kinetic Chain Exercises: An Analysis Using Computer Simulation. *The American Journal of Sports Medicine*, 29(4), 480–487. doi:10.1177/03635465010290041701
- Huang, N. E., Shen, Z., Long, S. R., Wu, M. C., Shih, H. H., Zheng, Q., Yen, N.-Ch., Tung, Ch. Ch., & Liu, H. H. (1998). The empirical mode decomposition and the Hilbert spectrum for nonlinear and non-stationary time series analysis. *Proceedings of the Royal Society of London. Series A: Mathematical, Physical and Engineering Sciences*, 454(1971), 903–995. doi:10.1098/rspa.1998.0193
- Jonak, J., Machrowska, A., Podgórski, J., & Bęc, J. (2016). Identification of the operating parameters for the mechanical system using EMD algorithm. *MATEC Web of Conferences*, 83, 05001. doi:10.1051/mateconf/20168305001
- Karpiński, R., Machrowska, A., & Maciejewski, M. (2019). Application of acoustic signal processing methods in detecting differences between open and closed kinematic chain movement for the knee joint. *Applied Computer Science*, 15(1), 36–48. doi:10.23743/acs-2019-03
- Kolotkov, D. Y., Anfinogentov, S. A., & Nakariakov, V. M. (2016). Empirical mode decomposition analysis of random processes in the solar atmosphere. *Astronomy & Astrophysics*, 592, A153. doi:10.1051/0004-6361/201628306

- Luque-Seron, J. A., & Medina-Porqueres, I. (2016). Anterior Cruciate Ligament Strain In Vivo: A Systematic Review. *Sports Health: A Multidisciplinary Approach*, 8(5), 451–455. doi:10.1177/1941738116658006
- Machrowska, A., & Jonak, J. (2018). xEMD procedures as a data – Assisted filtering method. *AIP Conference Proceedings*, 1922, 120007. doi:10.1063/1.5019122
- Maciejewski, M. (2015). Zastosowanie i ograniczenia technologii informacyjnych w diagnostyce medycznej. *Informatyka, Automatyka, Pomiary w Gospodarce i Ochronie Środowiska*, 1, 66–72.
- Maciejewski, M., Surtel, W., & Dzida, G. (2015). Human ECG signal parameters estimation during controlled physical activity. In R. S. Romaniuk (Ed.), *Proc. SPIE 9662, Photonics Applications in Astronomy, Communications, Industry, and High-Energy Physics Experiments* (96621P). doi:10.1117/12.2205811
- Powers, C. M., Bolgla, L. A., Callaghan, M. J., Collins, N., & Sheehan, F. T. (2012). Patellofemoral Pain: Proximal, Distal, and Local Factors—2nd International Research Retreat, August 31–September 2, 2011, Ghent, Belgium. *Journal of Orthopaedic & Sports Physical Therapy*, 42(6), A1–A54. doi:10.2519/jospt.2012.0301
- Sanchis-Alfonso, V. (2014). Holistic approach to understanding anterior knee pain. Clinical implications. *Knee Surgery, Sports Traumatology, Arthroscopy*, 22(10), 2275–2285. doi:10.1007/s00167-014-3011-8
- Sanchis-Alfonso, V., & Dye, S. F. (2017). How to Deal With Anterior Knee Pain in the Active Young Patient. *Sports Health: A Multidisciplinary Approach*, 9(4), 346–351. doi:10.1177/1941738116681269
- Witvrouw, E., Danneels, L., van Tiggelen, D., Willems, T. M., & Cambier, D. (2004). Open versus Closed Kinetic Chain Exercises in Patellofemoral Pain: A 5-Year Prospective Randomized Study. *The American Journal of Sports Medicine*, 32(5), 1122–1130. doi:10.1177/0363546503262187
- Yaslan, Y., & Bican, B. (2017). Empirical mode decomposition based denoising method with support vector regression for time series prediction: A case study for electricity load forecasting. *Measurement*, 103, 52–61. doi:10.1016/j.measurement.2017.02.007